

The axisymmetric shrink fit problem subjected to torsion

J.P. Lopes^{a,*}, D.A. Hills^a

^a*Department of Engineering Science, University of Oxford,
Parks Road, Oxford OX1 3PJ, United Kingdom*

Abstract

The problem of an elastic shaft fitted into an under-sized hole in an elastically identical body, the latter in the form of a half-space, has been studied when the assembly is subject to increasing and then subsequently reducing torque. The solution has been found as the superposition of a unilateral solution for an adhered contact pair and a set of ring dislocations along the contact interface to represent slip. The dislocations needed are prismatic (b_z) and twist or screw (b_θ), and by using continuous distributions of them the modified traction may be represented very effectively in a way which enables the local orthogonality requirement of slip to be followed rigorously. The residual interface tractions left when the applied torque has been completely removed are found. The whole calculation was carried out on a quasi-static basis.

Keywords: Axisymmetric, Contact, Shrink fit, Torsion, Orthogonality, Frictional slip, Plane/anti-plane slip

1. Introduction

The problem of a cylinder shrink fitted into an under-sized cavity arises in a number of engineering problems such as when a disk (pulley, gear etc) is shrink fitted onto a shaft, or in the domestic environment of, for example, a cork or stopper closure. The relationship between the degree of interference and the contact pressure generated in a plane problem has been known for a very long time and is associated with the name Lamé, but the presence of a free surface, where the contact terminates, produces interesting complicating three dimensional effects which can be solved in closed form [1]. The gradients along the axis of the shaft which the free surface induces means that axial shear tractions arise, and these have been shown [1] to be sufficiently severe for slip always to be present when the contact is formed, for realistic coefficients of friction.

The object of the present paper is to extend this solution to problems in which a torque is inserted at the free surface itself, and to see how this modifies the interfacial shear tractions present. Although the solution has relevance to engineering assemblies it also has relevance to the cork closure refereed to: a corkscrew is normally twisted and released before an axial force is applied, and this paper shows how a self-equilibrating residual interface shear traction is developed by the twisting action. Although the axial force part of the problem is not considered, it is clear that the torque pre-load will reduce the value of the axial force needed to achieve extraction of the cork.

The formulation presented in this work relies on two idealisations that might lead to gross approximations when applied to practical applications but have to be made due to the current state of knowledge of the tools for analytical modelling of shrink fit under partial slip.

The method used to introduce interfacial slip relies on the knowledge of the state of stress induced in a half-space by a ring dislocation lying in a plane parallel with the surface (kernel or core of the solution). In practical applications, the hub and the shaft might be made of different materials and this would imply knowing the kernel for a mismatched half-space, which is not available in the literature. We assume, therefore, that the hub and the shaft are made of the same material, and consider the case where the half-space is homogeneous [2].

In addition, the application of a torque is usually distributed over the surface of the shaft. However, a point torque was chosen to be applied because; (a) the solution was available in the literature in an elegant format for a homogeneous half-space [3], (b) the only mathematical singularity in the stress fields appears at the origin (away from the contact interface), (c) and it presents no intrinsic length dimension, i.e. it introduces no extra parameters in the model.

2. Shrink fit assembly

The stresses due to the shrink fit assembly (shown in Figure 1) are given by Paynter et al. [1] and are reproduced here. Upon assembly, an infinitely long oversized shaft of radius $a + \Delta_0$ is inserted in a hub with a cylindrical hole of radius a , present in an elastic half-space. Both the shaft and the hub have Poisson's ratio ν and Young's modulus

*Corresponding author

Email addresses: jhonatan.dapontelopes@eng.ox.ac.uk (J.P. Lopes), david.hills@eng.ox.ac.uk (D.A. Hills)

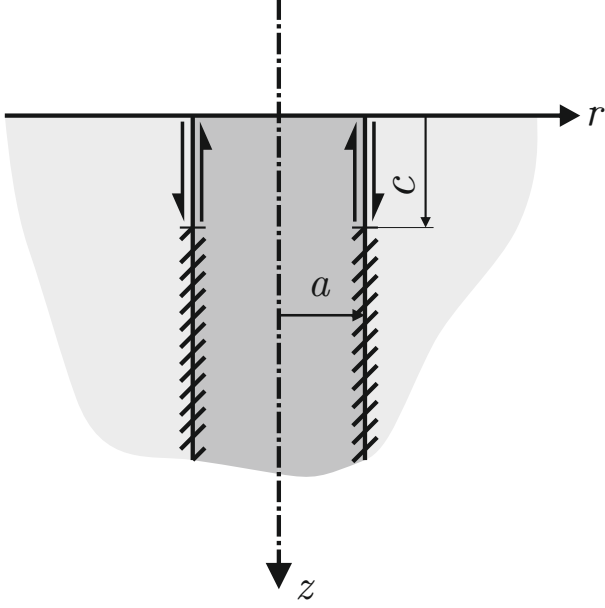


Figure 1: A semi infinite shaft of radius a in a half-space $z > 0$ subjected to shrink fit.

E. The assembly can be achieved by cooling the oversized shaft through a temperature differential ΔT until it fits in the hub and then letting it warm back up. This results in an induced radial strain ϵ^* in the shaft, given by

$$\epsilon^* = \frac{\Delta_0}{a} = \alpha \Delta T \quad (1)$$

where α is the coefficient of thermal expansion for the shaft.

If the coefficient of friction is sufficiently high to prevent any slip, the stresses σ_{ij}^{SF} at a point (r, z) , $z \geq 0$, are given by

$$\sigma_{rr}^{SF}(r, z) = \sigma_0 \left[a \left(P_{1,0;0}(\rho, \zeta) - z P_{1,0;1}(\rho, \zeta) + \frac{z}{r} P_{1,1;0}(\rho, \zeta) - \frac{\kappa - 1}{2r} P_{1,1;-1}(\rho, \zeta) \right) + \begin{cases} -1/2 & r \leq a \\ -a^2/(2r^2) & r > a \end{cases} \right] \quad (2)$$

$$\sigma_{rz}^{SF}(r, z) = \sigma_0 a z P_{1,1;1}(\rho, \zeta), \quad (3)$$

where $\sigma_0 = E \epsilon^*/(1 - \nu)$ is a reference axial stress and $P_{m,n;p}(\rho, \zeta)$ are Lipschitz-Hankel integrals, defined in Appendix A.

The third kind elliptic integrals present in the Lipschitz-Hankel integrals in eqs. (2) and (3) are singular when $(r, z) = (a, 0)$. For this point, we obtain the stress values by taking the limits as $z \rightarrow 0$, which give

$$\sigma_{rr}^{SF}(a, 0) = \sigma_0 \left(\nu - \frac{1}{2} \right) \quad (4)$$

$$\sigma_{rz}^{SF}(a, 0) = -\frac{\sigma_0}{\pi}. \quad (5)$$

For the stresses in eqs. (2) and (3) to be valid, they cannot violate the slip condition, i.e.

$$|\sigma_{rz}^{SF}(z)| \leq f \sigma_{rr}^{SF}(z) < 0 \quad z \geq 0. \quad (6)$$

However, Paynter et al. [1] show that a realistic coefficient of friction ($f \lesssim 1.0$) will result in the violation of eq. (6) and, consequently, the contact must be in partial slip.

Because the coefficient of friction is insufficient to maintain complete adhesion, a region of slip will develop when the assembly is put together, whose extent we wish to know. In order to satisfy slipping conditions, a modified solution can be developed by representing the tractions at the contact interface as a sum of the bilateral (adhered) solution together with a correction in the form of an integral representation of slip as a distribution of glide dislocations.

We emphasise that the introduction of dislocations is used only as a mathematical device to correct the tractions in the formulation as a distribution of strain nuclei. This does not mean that physical defects are being inserted in the micro-structure of the material. Detailed explanations of the method can be found in [4, 5].

The modelling of contact slip is achieved by introducing an axial glide dislocation loop $b_z(\xi)$ of radius a , placed at a depth ξ . This loop has a Burgers vector which is constant in magnitude and orientation so that it is of the Volterra kind and may be formed by making a path cut along the cylinder $r = a$ between the dislocation and the free surface of the half-space and sliding the outer wall with respect to the inner wall by a constant amount b_z . This will introduce tractions $\hat{\sigma}_{iz}(z)$, $i = r, z$, along the same path cut, given by

$$\hat{\sigma}_{iz}(z) = G_{ri}^z(z, \xi) b_z(\xi). \quad (7)$$

The influence functions $G_{ri}^z(z, \xi)$ are described as sums of Lipschitz-Hankel integrals, and for a half-space are given by Paynter et al. [2, 6] and in the Appendix A.

We can now write the contact pressure $p^{(0)}(z)$ and shear stress $q_{rz}^{(0)}(z)$ at the interface as

$$p^{(0)}(z) = \sigma_{rr}^{SF}(z) + \int_{slip} G_{rr}^z(z, \xi) B_z(\xi) d\xi \quad (8)$$

$$q_{rz}^{(0)}(z) = \sigma_{rz}^{SF}(z) + \int_{slip} G_{rz}^z(z, \xi) B_z(\xi) d\xi. \quad (9)$$

The slip condition requires that the shear stress must be limited by friction in the slip zone, i.e.

$$p^{(0)}(z) < 0 \quad (10)$$

$$q_{rz}^{(0)}(z) = -f p^{(0)}(z) \quad 0 \leq z \leq c \quad (11)$$

where f is the coefficient of friction between the shaft and the hole, and c the depth to which slip penetrates.

Substituting eqs. (8) and (9) into eq. (11), we have the following singular integral equation:

$$\int_0^c [G_{rz}^z(z, \xi) + f G_{rr}^z(z, \xi)] B_z(\xi) d\xi = -[\sigma_{rz}^{SF}(z) + f \sigma_{rr}^{SF}(z)] \quad 0 \leq z \leq c, \quad (12)$$

which can be solved using standard Gauss-Chebyshev quadrature [7, 4].

After solving eq. (12) for $B_z(\xi)$, the stresses can be recovered from integration (eqs. (8) and (9)) and the slip displacement is given by:

$$h_{rz}^{(0)}(z) = -\int_z^c B_z(\xi) d\xi. \quad (13)$$

3. Formulation of twist problem

After assembling the shrink fit, a point torque T is applied acting into the elastic half-space. In the cylindrical coordinate set of Figures 2a and 2b, the state of stress within the half-space is given by Chowdhury [3, 8], and the non-zero tractions arising on any cylindrical cut (an $r = \text{constant}$ surface), $\sigma_{ij}^T(r, z)$ are given by

$$\sigma_{r\theta}^T(r, z) = -\frac{3T}{4\pi} \left\{ \frac{rz}{(r^2 + z^2)^{5/2}} \right\} \quad (14)$$

$$\sigma_{z\theta}^T(r, z) = -\frac{3T}{4\pi} \left\{ \frac{r^2}{(r^2 + z^2)^{5/2}} \right\}. \quad (15)$$

A normalised variable γ is chosen as a measure of the shrink fit to applied torque stress ratio, given by

$$\gamma = \frac{T}{a^3 \sigma_0}. \quad (16)$$

Therefore, $\gamma = 0$ represents the contact assembly, i.e. only the shrink fit stresses are present. A positive γ implies that the shaft is being twisted clockwise (when looking from the free surface), while a negative γ represents the shaft being twisted anticlockwise.

Notice that, on any cylindrical cuts ($r = \text{constant}$ surfaces), the shrink fit assembly produces only q_{rz} shear stress, acting in the z direction, while the application of the torque results in a shear stress $q_{r\theta}$ in the θ direction, perpendicular to the direction of slip in the assembly.

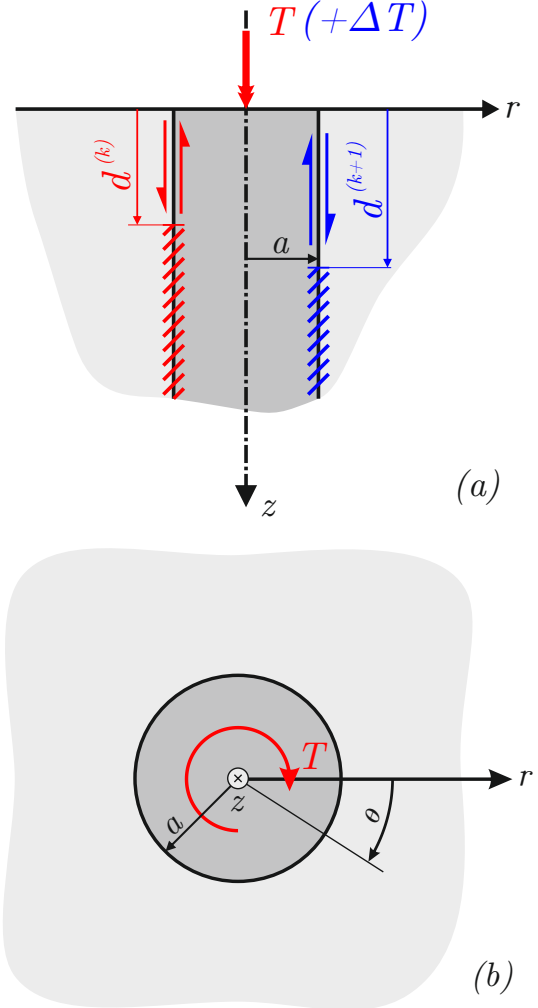


Figure 2: A semi-infinite shaft of radius a in a half-space $z > 0$ subjected to shrink fit. (a) State (k) on the left: the system holds a torque T . State $(k+1)$ on the right: an increment of torque ΔT is applied. (b) View from free surface showing a positive torque.

Close to the contact edge, q_{rz} acts as an ‘in-plane’ component of shear, while $q_{r\theta}$ represents an ‘anti-plane’ component. While over the whole contact these components are acting along a constant $r = a$ cylinder instead of a plane, we shall employ the nomenclature in-plane/anti-plane to reference the shear components $q_{rz}/q_{r\theta}$ respectively.

Because there are now two components of shear stress in perpendicular directions being applied to the bodies, the slip condition needs to be modified. In the stick zone, the total shearing traction at each point must be less than that needed to cause slip, i.e.

$$p(z) < 0, \quad [q_{rz}(z)]^2 + [q_{r\theta}(z)]^2 < [f p(z)]^2 \quad (17)$$

and in the slip zone, the total shearing traction is limited by friction:

$$p(z) < 0, \quad [q_{rz}(z)]^2 + [q_{r\theta}(z)]^2 = [f p(z)]^2. \quad (18)$$

In addition, the direction of the equivalent shearing traction must be such that it is collinear with, but opposed to, the slip velocity (orthogonality condition) [9]:

$$\frac{q_{r\theta}(z)}{q_{rz}(z)} = \frac{\dot{h}_{r\theta}(z)}{\dot{h}_{rz}(z)}, \quad (19)$$

where $\dot{h}_{ri}(z)$ represents the slip velocity in the direction $i = r, \theta$.

Consequently, it is necessary to solve the problem incrementally, to ensure that this condition is met instantaneously at each time step.

3.1. Incremental solution

In order to find the solution for a general time step $k+1$, we assume that we have a solution for the stresses and slip displacements for the shaft/hub system in the current step k , where the system holds a torque T . The solution at step k is characterized by the normal stress $p^{(k)}(\gamma, z)$, in-plane shear stress $q_{rz}^{(k)}(\gamma, z)$, in-plane tangential displacement $h_{rz}^{(k)}(\gamma, z)$, anti-plane shear stress $q_{r\theta}^{(k)}(\gamma, z)$ and anti-plane tangential displacement $h_{r\theta}^{(k)}(\gamma, z)$. It is also assumed that in this step a slip zone was developed, extending from $z = 0$ to a point $z = d^{(k)}$ (left side of Figure 2a).

When $k + 1 = 1$, the k state is defined as the shrink fit assembly, where $p^{(0)}(z)$, $q_{rz}^{(0)}$ and $h_{rz}^{(0)}(z)$ were obtained in Section 2, and $q_{r\theta}^{(0)} = h_{r\theta}^{(0)}(z) = 0$.

The solution for the state k must obey the slip condition, i.e. the magnitude of the shear stress must be limited by friction:

$$[\sigma_{rz}^{(k)}(\gamma, z)]^2 + [\sigma_{r\theta}^{(k)}(\gamma, z)]^2 = [f \sigma_{rr}^{(k)}(\gamma, z)]^2 \quad 0 \leq z \leq d^{(k)}. \quad (20)$$

An increment of torque $\Delta\gamma$ is applied, giving rise to the new state of stress $k + 1$. The torque in the system is now $\gamma + \Delta\gamma$. Due to a bilateral change caused by the increase in torque, the current solution (state k) is no longer valid, since it now violates the slip condition in eq. (20). We also expect the increment of torque to increase the size of the slip zone, which will now extend from $z = 0$ to a point $z = d^{(k+1)}$, where $d^{(k+1)} > d^{(k)}$ (right side of Figure 2a). This self-determining stick-slip transition point is an output of the problem. For simplicity, we shall drop the superscripts for the new state and write $d = d^{(k+1)}$, $p(z) = p^{(k+1)}(z)$, $q_{rz}(z) = q_{rz}^{(k+1)}(z)$ and $q_{r\theta}(z) = q_{r\theta}^{(k+1)}(z)$.

A modified solution for the new state $k + 1$ can be obtained as described in Section 2, by developing expressions for the tractions at the contact interface as the sum of the solution in the current state k together with a correction

in the form of an integral representation of slip as a distribution of glide dislocations. Because of the introduction of $\sigma_{r\theta}$ stresses, a screw glide dislocation loop $b_\theta(z)$ is needed in addition to the axial glide loop $b_z(z)$. The screw glide loop may be created by making a path cut along the cylinder $r = a$ between the dislocation and the free surface of the half-space and twisting the outer wall with respect to the inner wall by b_θ . This will introduce the following tractions along the same path cut

$$\hat{\sigma}_{i\theta}(z) = G_{\theta i}^\theta(z, \xi) b_\theta(\xi). \quad (21)$$

The influence functions $G_{\theta i}^\theta(z, \xi)$, $i = r, z$, are also described as sums of Lipschitz-Hankel integrals, and for a half-space are given by Sackfield et al. [10] and in the Appendix A.

The resulting normal $p(z)$, in-plane shear $q_{rz}(z)$ and anti-plane shear $q_{r\theta}(z)$ tractions along the contact interface for the current step are given by

$$p(\gamma + \Delta\gamma, z) = p^{(k)}(\gamma, z) + \int_0^d G_{rr}^z(z, \xi) B_z(\xi) d\xi, \quad (22)$$

$$q_{rz}(\gamma + \Delta\gamma, z) = q_{rz}^{(k)}(\gamma, z) + \int_0^d G_{rz}^z(z, \xi) B_z(\xi) d\xi \quad (23)$$

$$q_{r\theta}(\gamma + \Delta\gamma, z) = \tilde{\sigma}_{r\theta}(\gamma + \Delta\gamma, z) + \int_0^d G_{r\theta}^\theta(z, \xi) B_\theta(\xi) d\xi \quad (24)$$

where $B_i(\xi) = db_i/d\xi$, $i = z, \theta$ represents the dislocation density and $\tilde{\sigma}_{r\theta}(\gamma + \Delta\gamma, z)$ represents the sum of the anti-plane shear stress in the previous state $q_{r\theta}^{(k)}(\gamma, z)$ and the contribution due to the increase in torque $\sigma_{r\theta}^T(\Delta\gamma, z)$,

$$\tilde{\sigma}_{r\theta}(\gamma + \Delta\gamma, z) = q_{r\theta}^{(k)}(\gamma, z) + \sigma_{r\theta}^T(\Delta\gamma, z). \quad (25)$$

Equations (22) to (25) form the basis of the solution and integral equations may be generated to restore Signorini and orthogonality conditions.

In the closed, slipping region, the equivalent shearing traction must be limited by friction:

$$p(z) < 0 \quad [q(z)]^2 = [f p(z)]^2 \quad 0 \leq z \leq d, \quad (26)$$

where

$$q(z) = \sqrt{[q_{rz}(\gamma + \Delta\gamma, z)]^2 + [q_{r\theta}(\gamma + \Delta\gamma, z)]^2}. \quad (27)$$

In addition, the in-plane and anti-plane shear tractions must be subjected to the orthogonality condition (eq. (19)).

Even though the loading is quasi-static, there is still the need to correlate the application of the torque with the pseudo time derivatives:

$$\frac{dh(T, z)}{dt} = \frac{dT}{dT} \frac{dh(T, z)}{dT}. \quad (28)$$

Therefore, for a finite time step ΔT , we can approximate eq. (19) by

$$\frac{q_{r\theta}(z)}{q_{rz}(z)} = \frac{\Delta h_{r\theta}(z)}{\Delta h_{rz}(z)}. \quad (29)$$

Equations (26) and (29) form a system of non-linear singular integral equations with Cauchy kernels. There are two unknown functions to be determined, $B_z(z)$ and $B_\theta(z)$, and an unknown stick-slip transition point, d . However, obtaining a solution in this non-linear format is extremely difficult. Previous attempts at solving plane/anti-plane frictional problems involved the use of special elements of strain nuclei, such as triangular elements of dislocation densities [11, 12, 13, 14]. We propose, instead, a simple modification to the system that allows for an iterative solution using standard Gauss-Chebyshev quadrature devised by Erdogan et al. [7].

3.2. Numerical scheme

The angle of slip at each point $\alpha(z)$ can be given either as the ratio between the components of shear stress or the velocity components. Hence, each side of eq. (29) gives the tangent of the angle of slip $\alpha(z)$ at each point and we can rewrite the equation as:

$$\frac{q_{r\theta}(z)}{q_{rz}(z)} = \tan(\alpha(z)), \quad (30)$$

$$\frac{\Delta h_{r\theta}(z)}{\Delta h_{rz}(z)} = \tan(\alpha(z)). \quad (31)$$

Substitution of eq. (30) in eq. (26), together with eq. (31), leads to the following linear system of singular integral equations:

$$q_{rz}(z) = -f \cos(\alpha(z)) p(z), \quad (32)$$

$$q_{r\theta}(z) = -f \sin(\alpha(z)) p(z), \quad (33)$$

$$\frac{\Delta h_{r\theta}(z)}{\Delta h_{rz}(z)} = \tan(\alpha(z)). \quad (34)$$

Applying eqs. (22) to (24) to eqs. (32) to (34), gives

$$\begin{aligned} & \int_0^d \left[G_{rz}^z(z, \xi) + f \cos(\alpha(z)) G_{rr}^z(z, \xi) \right] B_z(\xi) d\xi + \\ & = - \left[q_{rz}^{(k)}(z) + f \cos(\alpha(z)) p^{(k)}(z) \right] \quad 0 \leq z \leq d \end{aligned} \quad (35)$$

$$\begin{aligned} & \int_0^d G_{r\theta}^\theta(z, \xi) B_\theta(\xi) d\xi + \\ & f \sin(\alpha(z)) \int_0^d G_{rr}^z(z, \xi) B_z(\xi) d\xi + \\ & = - \left[\tilde{\sigma}_{r\theta}(z) + f \sin(\alpha(z)) p^{(k)}(z) \right] \quad 0 \leq z \leq d. \end{aligned} \quad (36)$$

Owing to the nature of the functions present in eqs. (35) and (36), there is no hope of analytically inverting the integral equations. However, there are no explicit nonlinearities in them and, assuming that $\alpha(z)$ is known, the singular integral equations (SIE's) can be solved numerically, using Gauss-Chebyshev quadrature [7]. The two equations are imposed over one region ($0 \leq z \leq d$), and, as long as $B_z(z)$ and $B_\theta(z)$ can each be described by the same fundamental function (same behaviour at the ends of the interval), only one set of quadrature points is needed.

The first step in solving the SIE's is to put the integrals in standard form over the interval $[-1, 1]$. We choose the following substitution

$$s = \frac{2\xi}{d} - 1 \quad (37)$$

$$t = \frac{2z}{d} - 1 \quad (38)$$

$$(39)$$

which gives

$$\begin{aligned} & \int_{-1}^1 \left[G_{rz}^z(t, s) + f \cos(\alpha(t)) G_{rr}^z(t, s) \right] B_z(s) ds + \\ & = - \frac{2}{d} \left[q_{rz}^{(k)}(t) + f \cos(\alpha(t)) p^{(k)}(t) \right] \quad -1 \leq t \leq 1 \end{aligned} \quad (40)$$

$$\begin{aligned} & \int_{-1}^1 G_{r\theta}^\theta(t, s) B_\theta(s) ds + \\ & f \sin(\alpha(t)) \int_{-1}^1 G_{rr}^z(t, s) B_z(s) ds + \\ & = - \frac{2}{d} \left[\tilde{\sigma}_{r\theta}(t) + f \sin(\alpha(t)) p^{(k)}(t) \right] \quad -1 \leq t \leq 1. \end{aligned} \quad (41)$$

For the general form of the solution, the two dislocation densities must be bounded at both ends of the interval. Thus, we choose

$$B_z(s) = \phi_z(s) \sqrt{1-s^2} \quad (42)$$

$$B_\theta(s) = \phi_\theta(s) \sqrt{1-s^2} \quad (43)$$

and eqs. (40) and (41) become, in normalised form,

$$\begin{aligned} & \sum_{i=1}^N \left\{ \left[G_{rz}^z(t_j, s_i) + f \cos(\alpha(t_j)) G_{rr}^z(t_j, s_i) \right] W_i \phi_z(s_i) \right\} + \\ & = - \frac{2}{\pi d} \left[q^{(k)}(t_j) + f \cos(\alpha(t_j)) p^{(k)}(t_j) \right] \quad (44) \\ & \quad j = 1, \dots, N+1 \end{aligned}$$

$$\begin{aligned}
& \sum_{i=1}^N \left\{ \left[G_{r\theta}^\theta(t_j, s_i) \right] \phi_\theta(s_i) \right\} + \\
& \sum_{i=1}^N \left\{ \left[f \sin(\alpha(t_j)) G_{rr}^z(t_j, s_i) \right] \phi_z(s_i) \right\} \\
& = -\frac{2}{\pi d} \left[\tilde{\sigma}_{r\theta}(t_j) + f \sin(\alpha(t_j)) p^{(k)}(t_j) \right] \quad (45) \\
& \quad j = 1, \dots, N+1
\end{aligned}$$

where the integration points s_i , collocation points t_j and weights W_i for the quadrature are given as

$$s_i = \cos\left(\pi \frac{i}{N+1}\right) \quad i = 1, \dots, N \quad (46)$$

$$t_j = \cos\left(\frac{\pi}{2} \frac{2j-1}{N+1}\right) \quad j = 1, \dots, N+1 \quad (47)$$

$$W_i = \frac{1 - s_i^2}{2(N+1)}. \quad (48)$$

Equation (31) can be rewritten in terms of the displacements. Note that

$$\Delta h_{rz}(z) = -\int_z^d B_z(\xi) d\xi - h_z^{(k)}(z) \quad (49)$$

$$\Delta h_{r\theta}(z) = -\int_z^d B_\theta(\xi) d\xi - h_\theta^{(k)}(z). \quad (50)$$

which gives

$$\tan(\alpha(z)) = \frac{-\int_z^d B_\theta(\xi) d\xi - h_\theta^{(k)}(z)}{-\int_z^d B_z(\xi) d\xi - h_z^{(k)}(z)}. \quad (51)$$

Equation (34) can also be rewritten in a discretised form, viz.

$$\begin{aligned}
& \Delta h_{r\theta}(t_j) - \Delta h_{rz}(t_j) \tan(\alpha(t_j)) = 0, \\
& \quad j = 1, \dots, N+1.. \quad (52)
\end{aligned}$$

For a given angle of slip $\alpha(z)$, Equations (44), (45) and (52) form a system of $3N+3$ equations and $3N+2$ unknowns. These are the N values of $\phi_z(s_i)$, N values of $\phi_\theta(s_i)$, $N+1$ values of $\alpha(t_j)$ and the stick point d .

We can solve the system in eqs. (44), (45) and (52) by giving an initial guess for $\alpha(t_j)$ and d , solving the system in eqs. (44) and (45) for ϕ_z and ϕ_θ and using an iterative procedure to adjust $\alpha(t_j)$ and d to make sure that the solution satisfies the orthogonality condition in eq. (52).

4. Results

The problem was coded using the numerical processor MATLAB. Convergence was obtained using $N = 80$. A

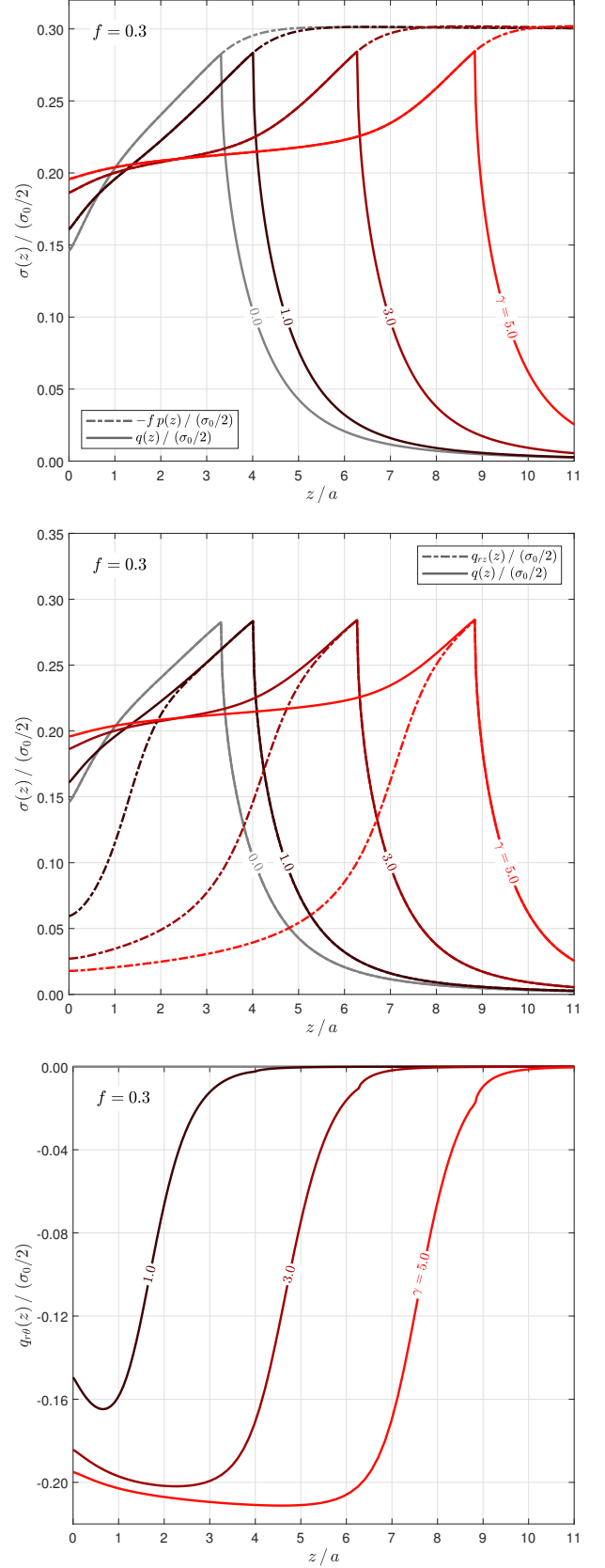


Figure 3: Normalised tractions at the contact interface for $f = 0.3$, $\gamma = 0.0, 1.0, 3.0$ and 5.0 . (a) Contact pressure and equivalent shear stress. (b) In-plane and equivalent shear stress. (c) Anti-plane shear stress.

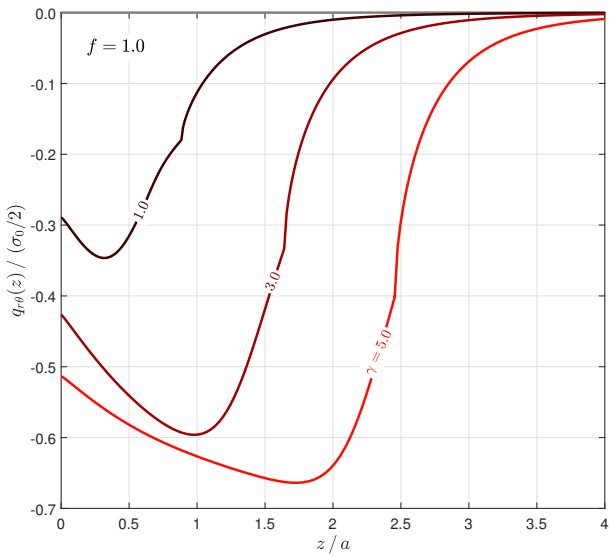
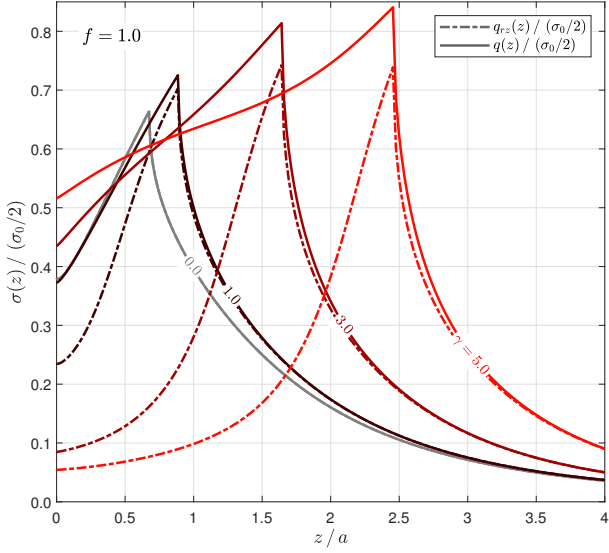
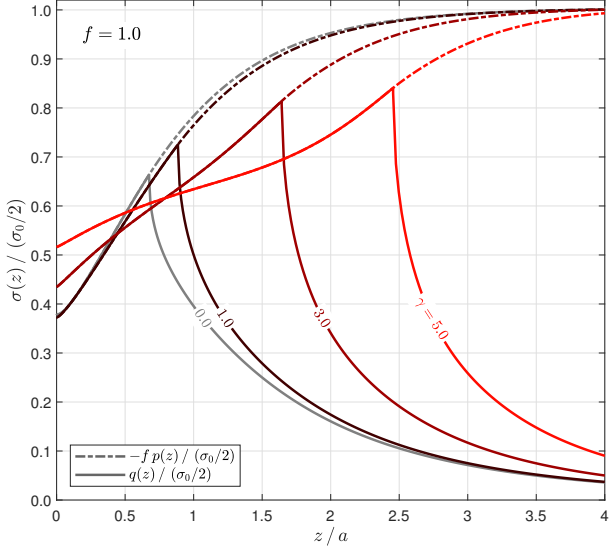


Figure 4: Normalised tractions at the contact interface for $f = 1.0$, $\gamma = 0.0, 1.0, 3.0$ and 5.0 . (a) Contact pressure and equivalent shear stress. (b) In-plane and equivalent shear stress. (c) Anti-plane shear stress.

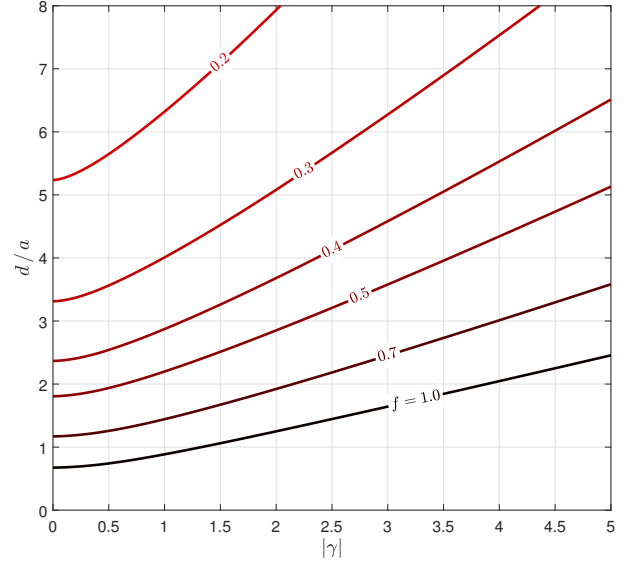


Figure 5: Normalised slip zone size d/a versus applied torque γ .

pseudo-time step of $\Delta\gamma = 0.05$ was used in all calculations. It was noted that changes in stresses and displacements for large γ was negligible when $\Delta\gamma$ was made smaller than 0.10. All the results presented in this paper are for $\nu = 0.3$.

Figures 3 and 4 show the tractions at the contact interface for $f = 0.3$ and 1.0 for $\gamma = 0.0, 1.0, 3.0$ and 5.0 , normalised by the reference stress $\sigma_0/2$. The stresses at the assembly are given by $\gamma = 0$ and represented by the curves in light grey.

Figures 3a and 4a show the variation with depth of the equivalent shear stress $q(z)$ (solid lines) together with the product of the contact pressure and the coefficient of friction $fp(z)$ (dash-dotted lines). Far away from the surface ($z \gg d$), the contact is fully stuck and, as expected, $|q(z)| < fp(z)$. As we move closer to the surface, the equivalent shear stress increases until it reaches $fp(z)$. At this point ($z = d$), the contact enters partial slip. For $0 \leq z \leq d$, the quantities $q(z)$ and $-fp(z)$ follow the same curve, since the contact is slipping. As γ increases, the slip-stick transition point d moves farther down, i.e. as more torque is applied to the shaft, it slips more deeply. Also, notice that the contact pressure itself at the surface changes significantly with the application of torque, increasing when γ increases. Even though the application of a torque produces no σ_{rr} stresses to change $p(z)$, the frictional behaviour of the contact results in a coupling effect, causing the pressure to change.

Figures 3b and 4b depict the variation with depth of the in-plane shear stress $q_{rz}(z)$ (dashed lines) together with the equivalent shear stress (solid lines). At assembly, $q_{r\theta}(z) = 0$ and, consequently, $q(z) = q_{rz}(z)$, which results in the two curves being the same. We notice that close to the surface the effect of the torque is more pronounced, and the difference between $q(z)$ and $q_{rz}(z)$ is higher. For greater depths, the effects of the torque vanish and the two curves converge. This is also shown in Figures 3c and 4c,

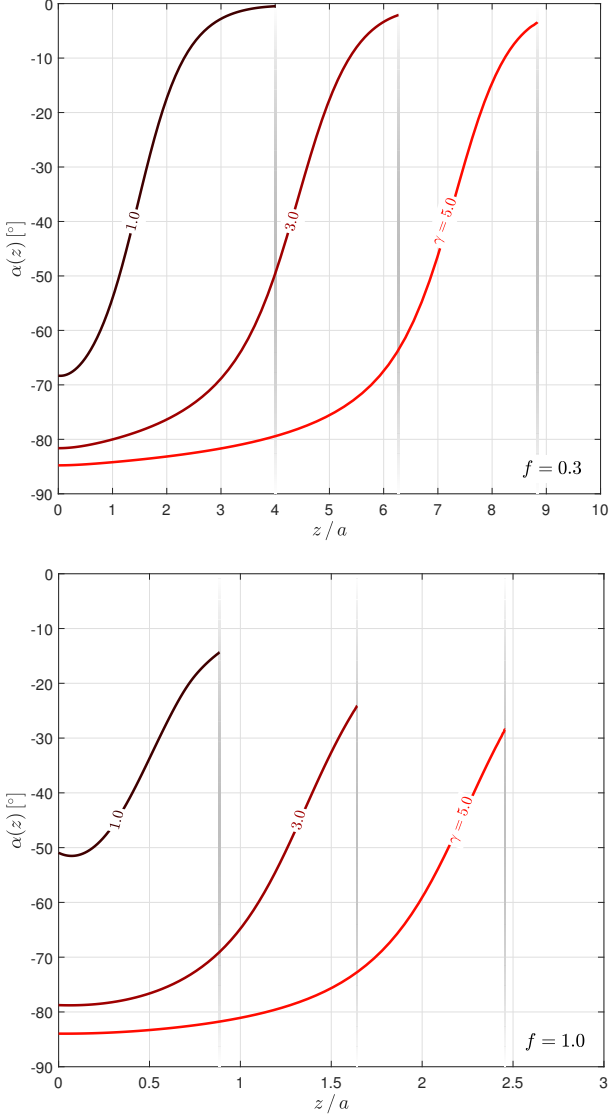


Figure 6: Angle of slip at the contact interface. (a) $f = 0.3$. (b) $f = 1.0$.

which represents the anti-plane shear stress $q_{r\theta}(z)$ as a function of z . We can see that $q_{r\theta}(z)$ is greater in magnitude closer to the surface and has a maximum inside the contact for both values of f and all γ .

Figure 5 shows the normalised slip zone size d/a as a function of the applied normalised torque γ for different values of coefficient of friction. As expected, as more torque is applied, the slip zone gets bigger. This effect is more pronounced for smaller coefficients of friction. Also, as expected, a higher value of f results in overall smaller slip zones than lower f . Furthermore, d/a is symmetric in γ , i.e. applying a negative torque would result in the same value of d/a . Since the shaft is semi-infinite, a finite torque can never cause spin, as it would require overcoming an infinite shear force.

Figure 6 depicts the angle of slip $\alpha(z)$ at the contact interface for $f = 0.3$ and 1.0 . The vertical lines represent

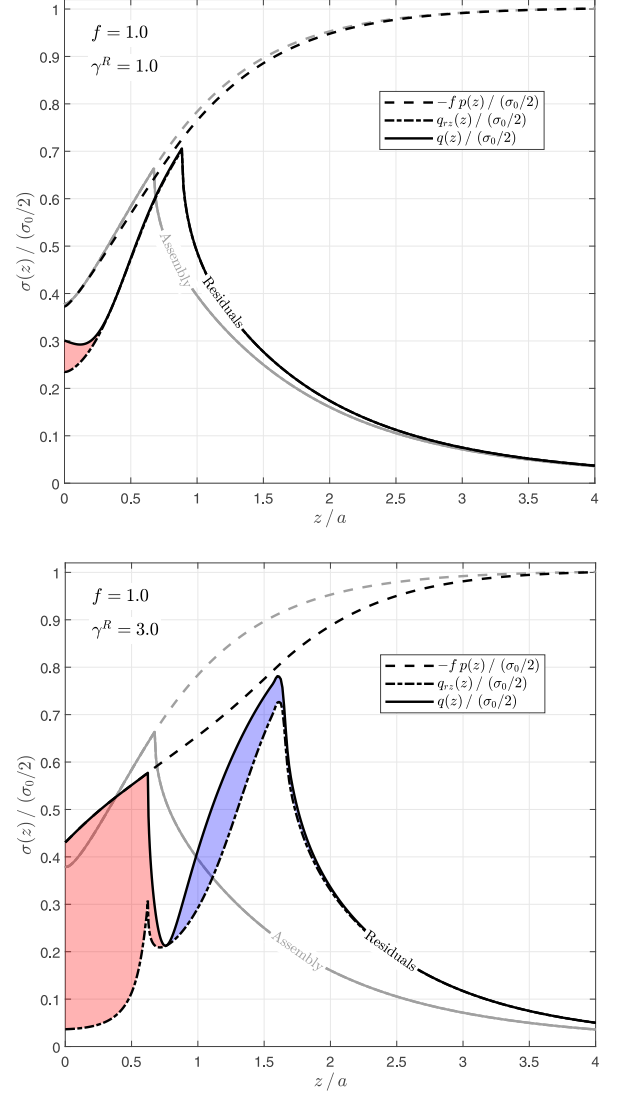


Figure 7: Normalised residual stresses at the contact interface for $f = 1.0$. (a) After applying $\gamma^R = 1.0$. (b) After applying $\gamma^R = 3.0$.

the normalised slip-stick transition points (d/a). For the shrink fit assembly ($\gamma = 0$), since there is no q_{rt} stress, slip is only in-plane and, consequently, the angle of slip is 0° throughout the slip zone. Notice that, as expected, close to the surface $\alpha(z)$ is higher and closer to -90° , since $q_{r\theta}$ is dominant and results in slip being predominantly in the anti-plane direction. However, because the shrink fit assembly results in the development of an in-plane q_{rz} stress, slip can never be purely in the anti-plane direction ($\alpha(z) = \pm 90^\circ$) for $0 \leq z \leq c$. This can be seen in Figure 6b, for $f = 1.0$ and $\gamma = 5.0$. Even though a considerable amount of torque is being applied, $\alpha(z)$ presents an asymptotic behaviour close to the surface, and it does not reach -90° . In addition, at the slip-stick transition point, the anti-plane shear stress is not required to be zero, as shown in Figures 3c and 4c. Hence, $\alpha(d)$ will not necessarily be equal to zero.

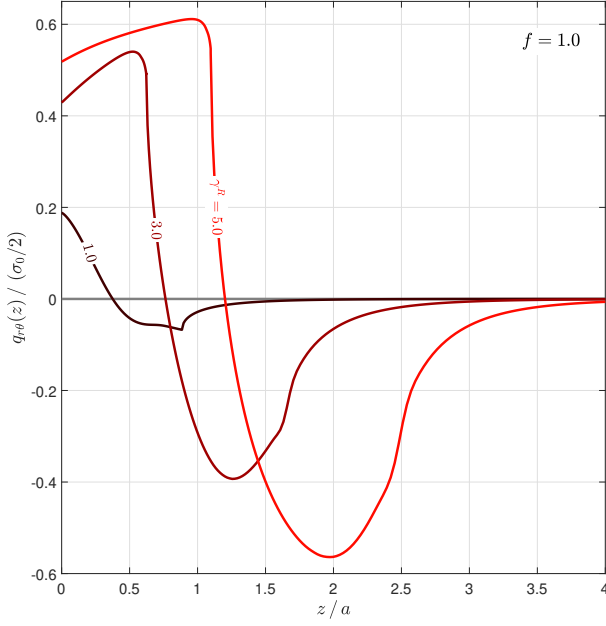


Figure 8: Normalised residual anti-plane stress at the contact interface.

4.1. Residual stresses

The next step in the analysis is to look at the residual stresses when a torque is monotonically applied to the system and subsequently relaxed. After assembling the shaft/hub system, a torque $\gamma = \gamma^R$ is monotonically applied. Subsequently, the torque is released (equivalent to applying $\gamma = -\gamma^R$), until the system is back to a no net torque state.

In the loading phase ($|\gamma|$ increasing), the slip zone size will extend from 0 to d and increase as γ increases. When γ is a maximum, d/a will be a maximum as well. As soon as the torque starts to decrease, the contact will stick everywhere instantaneously. As $|\gamma|$ decreases even further, new regions of slip will develop in the contact.

For simplicity, we shall consider only two cases, when the coefficient of friction is high ($f = 1.0$, Figure 7). In Figure 7a, a torque of $\gamma^R = 1.0$ is applied and then relaxed. In this case, after reaching the maximum torque, the contact sticks everywhere instantaneously, as soon as the torque starts to decrease. After unloading the torque completely, the final state is fully stuck. The curves in light grey represent the stresses at assembly, when no torque was applied, while the black curves represent the residual stresses. Notice that the equivalent shear stress is everywhere smaller than $-fp(z)$. Even though the two states represent no net torque, upon assembly the contact slips from $z = 0$ until $0.674a$, while this new state is completely stuck. There is also a considerable difference in the equivalent shear stress but not a lot of variation in contact pressure. We also note that the point where the shear stress peaks moved farther inside the contact.

In Figure 7b, a higher value of torque $\gamma^R = 3.0$ is applied and later relaxed. Similarly to the previous case,

the contact sticks everywhere as soon as the torque starts to decrease. However, as γ decreases, the equivalent shear stress close to the surface increases and results in violation of the slip condition. A new slip zone is formed, extending from $z = 0$ to $z = 0.620a$. After unloading the torque completely, the new state is now in partial slip but in a different configuration from assembly. The contact pressure and equivalent shear are significantly different from assembly.

The shaded areas in Figure 7 highlight the locked-in anti-plane shear stress $q_{r\theta}$. Because all states hold no net torque, the integral of $q_{r\theta}(z)$ over the surface area of the shaft must be zero. The red shaded areas represent the places where $q_{r\theta}(z) > 0$, while the blue shaded areas represent $q_{r\theta}(z) < 0$. In both figures, the areas are the same. In Figure 7a, the blue area is ‘hidden’ between the $q(z)$ and $q_{rz}(z)$ curves, which are very similar but not exactly the same. This is shown more clearly in Figure 8.

5. Conclusions

A solution was obtained for the tractions, displacements and geometric parameters for an oversized shaft shrink fitted to an elastically identical hub and subjected to torsion. Due to the torque, there are in-plane and anti-plane components of shear and, consequently, an incremental solution was needed.

It was shown that the problem exhibits considerable frictional coupling. Even though the torsion of the shaft does not explicitly induce σ_{rz} and σ_{rr} stresses, the solution shows that the contact pressure and in-plane shear stress are significantly affected by the application of the torque.

In addition, it was shown that in monotonic loading the size of the slip zone is proportional to the magnitude of the applied torque.

Finally, when unloading the system back to zero net torque it was shown that the residual stresses are history dependent. Although the final state represents no net torque, it still had locked-in anti-plane shear stress.

Acknowledgements

J. L. gratefully acknowledges the financial support of Christ Church Oxford, Rolls Royce PLC and Coordenação de Aperfeiçoamento de Pessoal de Nível Superior - CAPES.

References

- [1] R. Paynter, D. Hills, J. Barber, Features of the stress field at the surface of a flush shrink-fit shaft, Proceedings of the Institution of Mechanical Engineers, Part C: Journal of Mechanical Engineering Science 223 (10) (2009) 2241–2247.
- [2] R. Paynter, D. Hills, The effect of path cut on Somigliana ring dislocations in a half-space, International Journal of Solids and Structures 46 (2) (2009) 412–432.
- [3] K. Chowdhury, Solution of the problem of a concentrated torque on a semi-space by similarity transformations, Journal of Elasticity 13 (1) (1983) 87–90.

- [4] D. Hills, P. Kelly, D. Dai, A. Korsunsky, Solution of crack problems: the distributed dislocation technique, Vol. 44 of Solid Mechanics and Its Applications, Springer Netherlands, Dordrecht, 2013.
- [5] M. Comninou, D. Schmueser, J. Dundurs, Frictional Slip Between a Layer and a Substrate Caused by a Normal Load, International Journal of Engineering Science 18 (9) (1980) 131–137. doi:10.1016/0020-7225(80)90115-9.
- [6] J. Lopes, D. Hills, Ring cracks at the surface of a half-space, Engineering Fracture Mechanics 194 (2018) 105–116.
- [7] F. Erdogan, G. D. Gupta, T. Cook, Numerical solution of singular integral equations, in: Methods of analysis and solutions of crack problems, 1973, pp. 368–425.
- [8] C. Chow, F. Yang, On the solution of a concentrated torque on an orthotropic half-space, International Journal of Engineering Science 28 (9) (1990) 871–874.
- [9] J. Barber, Contact Mechanics, Solid Mechanics and Its Applications, Springer International Publishing, 2018.
- [10] A. Sackfield, J. Barber, D. Hills, C. Truman, A shrink-fit shaft subject to torsion, European Journal of Mechanics-A/Solids 21 (1) (2002) 73–84.
- [11] H. Qiu, D. Hills, D. Nowell, D. Dini, Skew sliding of an elastic cylinder: An investigation of convection in contact, International Journal of Mechanical Sciences 50 (2) (2008) 293–298.
- [12] H. Qiu, D. Dini, D. Hills, Torsional contact of an elastic flat-ended cylinder, Journal of the Mechanics and Physics of Solids 56 (12) (2008) 3352–3362.
- [13] H. Qiu, D. Hills, D. Dini, An investigation of convection effects in complete and almost complete contact problems, European Journal of Mechanics-A/Solids 28 (4) (2009) 680–687.
- [14] R. Bentall, K. Johnson, An elastic strip in plane rolling contact, International Journal of Mechanical Sciences 10 (8) (1968) 637–663.
- [15] G. Eason, B. Noble, I. N. Sneddon, On certain integrals of Lipschitz-Hankel type involving products of Bessel functions, Philosophical Transactions of the Royal Society of London A: Mathematical, Physical and Engineering Sciences 247 (935) (1955) 529–551.
- [16] R. Paynter, D. Hills, A. Korsunsky, The effect of path cut on Somigliana ring dislocation elastic fields, International Journal of Solids and Structures 44 (2) (2007) 6653–6677.

Appendix A. State of stress induced by circular edge dislocation loops

Appendix A.1. Axial prismatic dislocation

Consider a glide axial dislocation loop of radius a at a depth d and being observed at a position (r, z) in a cylindrical coordinate system, with a Burgers vector component b_z . The stress fields at a position (r, z) are given by

$$\sigma_{iz}^z(r, z) = G_{iz}^z(r, z, d) b_z(a) \quad i = r, z. \quad (\text{A.1})$$

The influence functions $G_{iz}^z(\rho, \zeta, \delta)$ ($i = r, z$) for the glide dislocation in a half-space are given as [2]:

$$G_{zz}^z(\rho, \zeta, \delta) = \frac{2\mu}{a(\kappa + 1)} \left[-J_{1,0;1} + I_{1,0;1} - (\zeta - \delta) J_{1,0;2} - (\zeta + \delta) I_{1,0;2} + 2\zeta \delta I_{1,0;3} \right] \quad (\text{A.2})$$

$$G_{rz}^z(\rho, \zeta, \delta) = \frac{2\mu}{a(\kappa + 1)} \left[-(\zeta - \delta) J_{1,1;2} + (\zeta - \delta) I_{1,1;2} - 2\zeta \delta I_{1,1;3} \right] \quad (\text{A.3})$$

where ρ , ζ and δ are the normalised coordinates, given by

$$\rho = r/a, \quad \zeta = z/a, \quad \delta = d/a, \quad (\text{A.4})$$

μ is the modulus of rigidity and κ is the Kolosov's constant.

The axial dislocation loop does not induce shear stresses in the θ direction, i.e. $G_{\theta z}^z(\rho, \zeta, \delta) = 0$.

Appendix A.2. Screw dislocation

Consider a glide screw dislocation loop of radius a at a depth d with a Burgers vector component b_θ and being observed at a position (r, z) in a cylindrical coordinate system. The stress field at a position (r, z) is given by

$$\sigma_{i\theta}^\theta(r, z) = G_{i\theta}^\theta(r, z, d) b_\theta(a) \quad i = r, z. \quad (\text{A.5})$$

The influence functions $G_{r\theta}^\theta(\rho, \zeta, \delta)$ ($i = r, z$) for the glide dislocation in a half-space are given as [10]:

$$G_{r\theta}^\theta(\rho, \zeta, \delta) = \frac{\mu a}{2} \left[J_{0,2;1} - 2J_{1,2;0} - (I_{0,2;1} - 2I_{1,2;0}) \right] \quad (\text{A.6})$$

$$G_{z\theta}^\theta(\rho, \zeta, \delta) = \frac{\mu a}{2} \left[J_{1,2;1} - I_{1,2;1} \right] \quad (\text{A.7})$$

Appendix A.3. Lipschitz-Hankel integrals

In the influence functions, the terms $J_{n,p;q}$ and $I_{n,p;q}$ represent Lipschitz-Hankel integrals. The standard definition for these functions is as an integral of the product of Bessel functions ($J_i(\cdot)$), an exponential term and a power term. Using normalised coordinate variables, it is given as [15]

$$P_{\mu,\nu;\lambda}(\rho, \zeta) = \int_0^\infty J_\mu(t) J_\nu(\rho t) e^{-\zeta t} t^\lambda dt. \quad (\text{A.8})$$

In this paper, the follow definition is applied:

$$J_{n,p;q} = P_{n,p;q}(\rho, \zeta - \delta) \quad (\text{A.9})$$

$$I_{n,p;q} = P_{n,p;q}(\rho, -\zeta - \delta) \quad (\text{A.10})$$

The Lipschitz-Hankel integrals needed in the paper are given by Paynter et al. [16, 2] and are available in MATLAB in [6].